New model for the field-aligned distribution of magnetospheric plasma related to the characteristic of dispersive Alfvén waves

齋藤幸碩 [1]、加藤雄人 [1]、木村智樹 [2]、川面洋平 [3,1]、熊本篤志 [1]

1：東北大学大学院理学研究科地球物理学専攻

2：東京理科大学理学部第一部物理学科

3：東北大学学際科学フロンティア研究所

木星探査機 Juno の観測により、木星メインオーバルにて数百 eV から数百 keV までの幅広いエネルギー帯におけるオーロラ電子降下が確認された[Mauk et al., 2017]。観測された電子のエネルギー分布ならびにピッチ角分布から、分散性 Alfvén 波(DAWs)による電子加速が木星におけるオーロラ形成過程において重要な役割を果たしていることが示唆された[Saur et al., 2018]。DAWs による電子加速過程の重要性が高まる一方で、電子加速が効率的に生じる領域や、加速エネルギーの上限値を決める主要因については未解明の問題が残されている。

DAWs による電子加速過程を考察するためには、DAWs の特性、すなわち分散関係を定める背景プラズマの数密度と圧力の空間分布を明らかにする必要がある。背景プラズマの空間分布に関する過去の研究では、数密度分布に関する理論・経験モデルや圧力分布に関する理論モデル[e.g., Angerami and Thomas, 1964; Phipps et al., 2018]が提案されてきた。一方で、温度分布が数密度分布とは独立に与えられるなど、数密度と圧力の分布をの双方を矛盾なく記述する理論モデルは提案されていない。以上の背景の下、本研究では、磁力線に沿った数密度と圧力の分布を速度分布関数に基づき求める理論モデル Plasma Distribution Solver (PDS)を開発した[Saito et al., submitted]。PDS は Static Vlasov Code (SVC) [Ergun et al., 2000; Su et al., 2003; Matsuda et al., 2010]を基に開発された。SVC は、プラズマの速度空間上の accessibility [e.g., Persson, 1966; Chiu and Schulz, 1978]を考慮して、速度分布関数から磁力線沿いの数密度分布を求める理論モデルである。我々は SVC における速度分布関数の空間変化の与え方を再検討して、適切な実装を図ることでより現実的なプラズマ分布を求めることを可能にし、さらにその速度分布関数から圧力を計算した。

PDS を木星-イオ系に適用することによって判明したこととして、以下の 2 点を報告する。

(1) PDS とその先行研究である SVC の各々から得られる木星-イオ系プラズマ数密度分布を比較した結果、分布の傾向は異なり、特に auroral cavity では、PDS では$2\ \mathrm{cm}^{-3}$で一定になる一方で、SVC では$0.5{\sim}6\ \mathrm{cm}^{-3}$の間で磁束密度に比例して変化する様相が示された。この違いは、PDS と SVC における速度分布関数の取り扱いの違いによる影響を顕著に示すものである。

(2) PDS によって求めた数密度分布から Alfvén 速度を算出し、イオから木星電離圏に到達するまでの時間を算出したところ、370 秒と見積もられた。したがって、Alfvén 波の伝播を解く際に PDS の解を背景場として用いる場合、少なくともこの時間スケールでは境界条件が変動しないという仮定を用いることと等価となる。

PDS はその適用条件の範囲で、系外を含む惑星磁場環境におけるプラズマ分布を求めることができるモデルである。PDS によって数密度、流速、プラズマ圧の空間分布を算出できることから、Alfvén 速度や電流密度、プラズマβなどの物理量を求めることができる。このことから、オーロラ電子加速過程や磁気圏-電離圏結合などの問題の解明に PDS を活かすことが可能であり、そして惑星大気の加速過程や系外を含む惑星一般のプラズマ分布の理解へとつながるものであると期待する。

New model for the field-aligned distribution of magnetospheric plasma related to the characteristics of dispersive Alfvén waves

K. Saito[1], Y. Katoh[1], T. Kimura[2], Y. Kawazura[3,1], and A. Kumamoto[1]

[1] Department of Geophysics, Graduate School of Science, Tohoku University.

[2] Department of Physics, Faculty of Science Division I, Tokyo University of Science.

[3] Frontier Research Institute for Interdisciplinary Sciences, Tohoku University.

e-mail: koseki.saito@stpp.gp.tohoku.ac.jp

SPS2022 おひさま#1 2022/02/09 10:32-10:49

Outline

Developing a theoretical model, "Plasma Distribution Solver (PDS),"
to calculate the field-aligned plasma number density and pressure profiles.

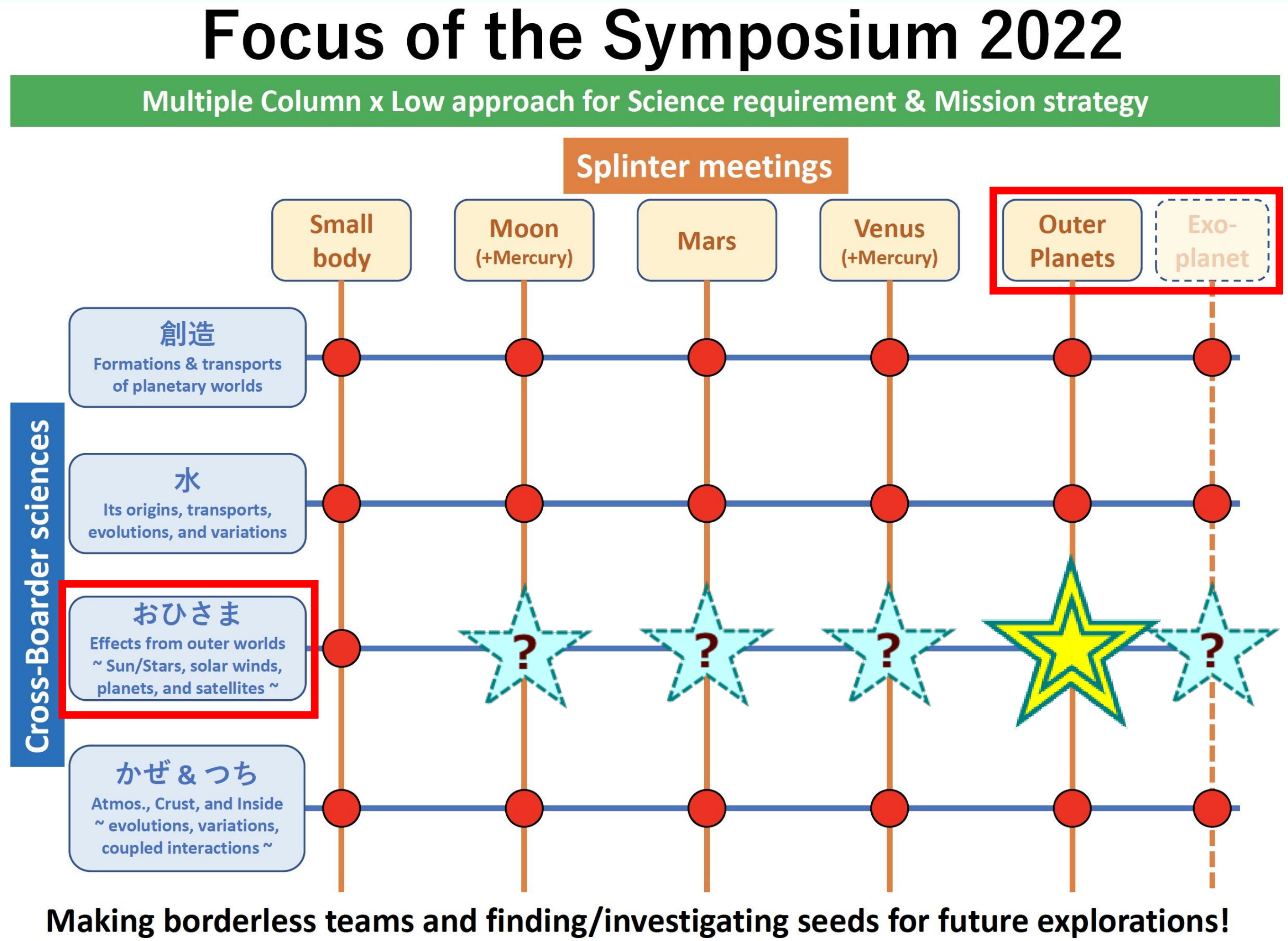

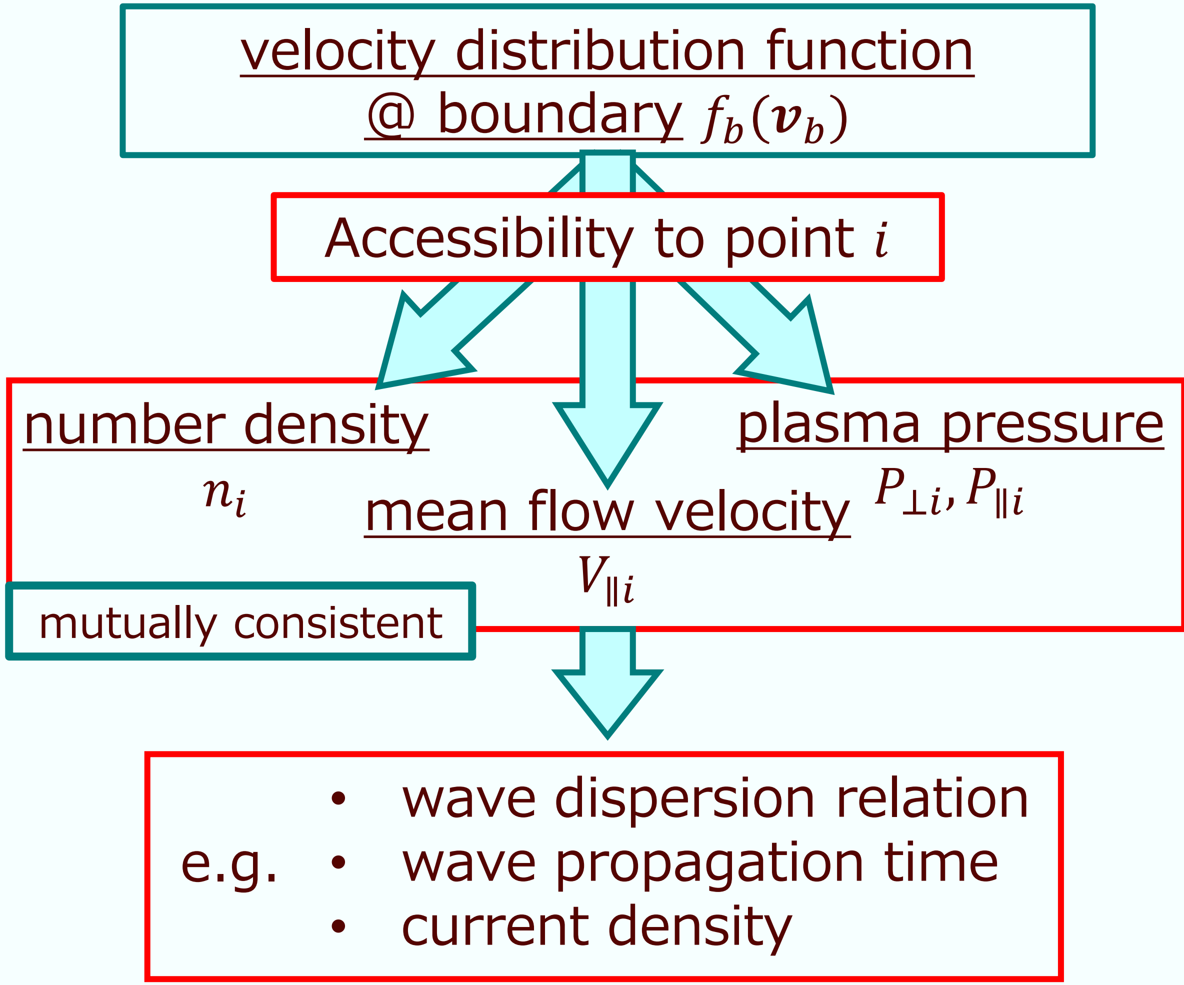

1. Introduction

Dispersive Alfvén waves

Jupiter-Io

~ several tens keV

electron energy [keV]

pitch angle [degree]

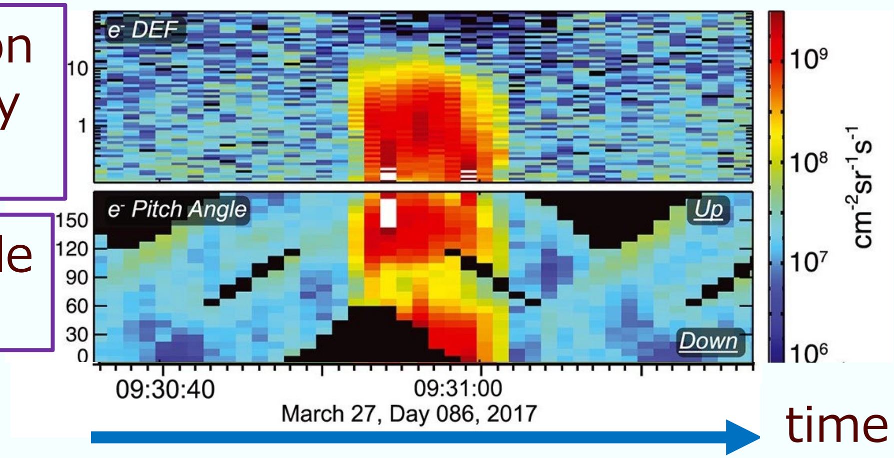

[Szalay et al., 2018]

Alfvenic acceleration
- e⁻ energy distribution

→ **broadband distribution from low to high.**

Jupiter main oval

~ 400 keV

[Mauk et al., 2017]

Dispersive Alfvén wave (DAW):

$k_\perp^{-1}$ is short $(k_\perp^{-1} \sim d_\mathrm{e}, \rho_\mathrm{i}, \rho_s)$ $(k_\parallel \ll k_\perp)$

(electron inertial length or ion Larmor radius)

$E_\parallel$ of DAWs accelerates electrons

Dispersion relation

$$\omega^2 = k_\parallel^2 v_\mathrm{A}^2 \frac{1 + k_\perp^2 \rho_s^2}{1 + k_\perp^2 d_\mathrm{e}^2}$$

[Streltsov and Lotko, 1995]

What are the main factors which determine the upper energy limits?

$k_{\parallel,\perp}$: parallel/perp wave number, ω: wave frequency, $\boldsymbol{E}$: electric field, $\boldsymbol{B}$: magnetic flux density, $\boldsymbol{v}$: velocity, $\boldsymbol{J}$: current density, v_A: Alfven speed, d_e: electron inertial length, $\boldsymbol{P}_e$: electron pressure, ρ_i: ion thermal Larmor radius, ρ_s: ion acoustic gyroradius, m_e: electron mass, n_e: electron number density, e: elementary charge

Background plasma settings

Alfven speed $v_A := \frac{Bc}{\sqrt{B^2 + c^2 \mu_0 \sum_i n_i m_i}}$

electron inertial length $d_e := c\sqrt{\frac{\varepsilon_0 m_e}{n_e e^2}}$

ion acoustic gyroradius $\rho_s := \frac{\sqrt{2 m_i P_{\perp e}}}{\zeta_i e B \sqrt{n_e}}$

The characteristics of DAW are determined by number density n and pressure P.

⇨ How do we obtain these profiles?

Static Vlasov Code (SVC)
[Ergun et al., 2000; Su et al., 2003; Matsuda et al., 2010]

The number density is theoretically obtained from the accessibility and the velocity distribution function f_i.

⇨ We can extend SVC to also obtain the mean flow velocity $V_\parallel$ and pressure P by integrating the velocity distribution function.

However, they assumed $f_i(\boldsymbol{v}_i) = f_b(\boldsymbol{v}_b)$.
We can improve the handling of spatial variations in the velocity distribution function.

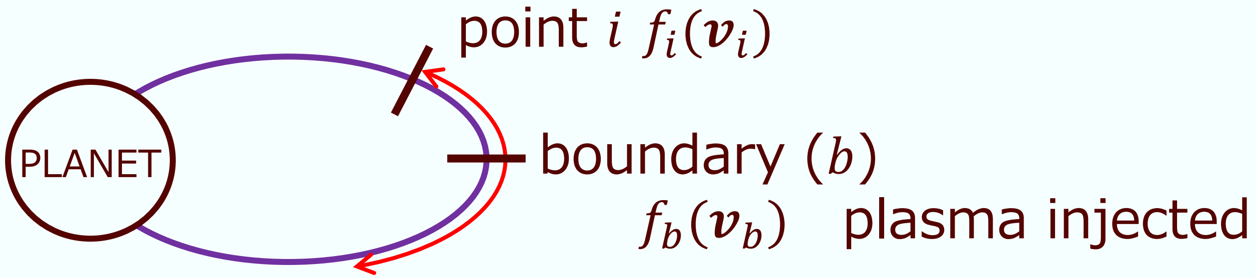

c: speed of light, μ_0: magnetic constant, ε_0: electric constant,
n_i: ion number density, m_i: ion mass, ζ_i: ion charge number,
$P_{\perp e}$: electron pressure perpendicular to the field line

Purpose

Clarifying the mechanism of electron acceleration by DAWs.
Evaluating how the plasma distribution affects this acceleration.

Main Objective

Developing a theoretical model to determine
the mutually consistent number density and pressure spatial distributions.

Purpose

we report

- Developing a theoretical model, "Plasma Distribution Solver (PDS),"
  to calculate the field-aligned plasma profile based on SVC.
- Applying PDS to the Jupiter-Io system
- Comparing with SVC

2. Development of Plasma Distribution Solver

Model and calculation method

Boundary/initial conditions

Z_s: number density at the boundary
$T_{\perp/\parallel\, s}$: temperature at the boundary
$\{\phi_i^0\}$: initial electrostatic potential profile (iteration)

i: spatial grid point ($-N \sim N$), s: plasma species

boundary:
Jovian ionospheric ends & Io

Velocity distribution function

Assuming as bi-Maxwellian at the boundary (b)

$$f_{sb}(v_{\perp b}, v_{\parallel b}) = \frac{Z_s}{\frac{2\pi T_{\perp s}}{m_s}\sqrt{\frac{2\pi T_{\parallel s}}{m_s}}} \exp\left(-\frac{m_s v_{\perp b}^2}{2T_{\perp s}}\right) \exp\left(-\frac{m_s v_{\parallel b}^2}{2T_{\parallel s}}\right)$$

- **Number density**

$$n_{si} = \iint_{\boldsymbol{v}_{si}} f_{sb}(v_{\perp b}, v_{\parallel b})\, 2\pi v_{\perp b} \mathrm{d}v_{\perp b} \mathrm{d}v_{\parallel b}$$

- Flow velocity (parallel)

$$V_{\parallel si} = \frac{1}{n_{si}} \iint_{\boldsymbol{v}_{si}} v_{\parallel i}\, f_{sb}(v_{\perp b}, v_{\parallel b}) 2\pi v_{\perp b} \mathrm{d}v_{\perp b} \mathrm{d}v_{\parallel b}$$

- **Plasma pressure**

$$P_{\perp si} = \frac{1}{2} m_s \iint_{\boldsymbol{v}_{si}} v_{\perp i}^2\, f_{sb}(v_{\perp b}, v_{\parallel b}) 2\pi v_{\perp b} \mathrm{d}v_{\perp b} \mathrm{d}v_{\parallel b}$$

$$P_{\parallel si} = m_s \iint_{\boldsymbol{v}_{si}} (v_{\parallel i} - V_{\parallel si})^2 f_{sb}(v_{\perp b}, v_{\parallel b}) 2\pi v_{\perp b} \mathrm{d}v_{\perp b} \mathrm{d}v_{\parallel b}$$

$$P_{si} = \frac{2P_{\perp si} + P_{\parallel si}}{3}$$

Accessibility

On the velocity space at the boundary,

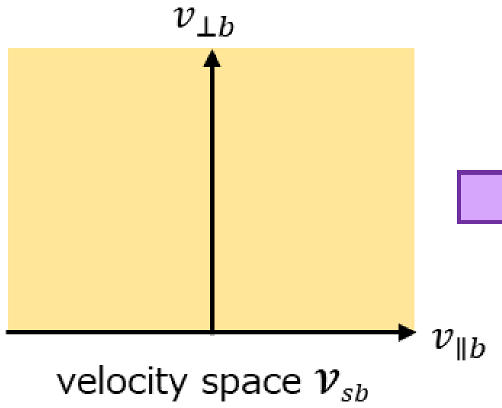

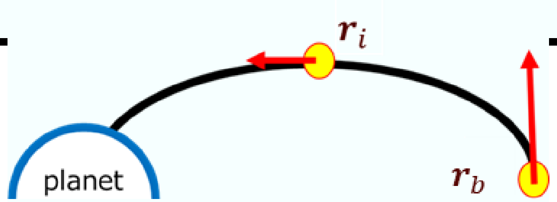

Energy conservation:

$$U_{sb} + \mu B_b + \frac{1}{2} m_s v_{\parallel b}^2 = U_{si} + \mu B_i + \frac{1}{2} m_s v_{\parallel i}^2$$

1st adiabatic invariant:

$$\mu = \frac{m_s v_{\perp b}^2}{2B_b} = \frac{m_s v_{\perp i}^2}{2B_i}$$

Velocity space in which particles arriving at grid point i

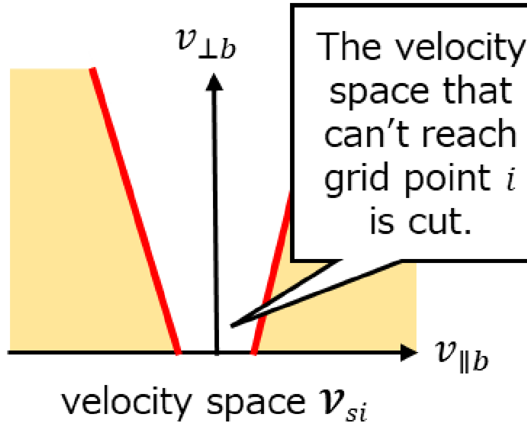

U_{si}: potential energy, $\boldsymbol{v}_{si}$: accessible velocity space at the boundary

Plasma Distribution Solver

Where and how many particles exist in velocity space at the boundary that can reach point i?

→ $f_b(\boldsymbol{v}_b)\mathrm{d}\boldsymbol{v}_b = f_i(\boldsymbol{v}_i)\mathrm{d}\boldsymbol{v}_i$

consideration of changes in the velocity space associated with the spatial change

$$n_i = \int_{\boldsymbol{\Omega}_i} \mathrm{d}\boldsymbol{v}_i\, f_i(\boldsymbol{v}_i) = \int_{\boldsymbol{\nu}_i} \mathrm{d}\boldsymbol{v}_b\, f_b(\boldsymbol{v}_b)$$

PDS integrate $f_b(\boldsymbol{v}_b)$ over $\boldsymbol{\nu}_i(\boldsymbol{v}_b)$ in velocity space at the boundary.

$$n_i = \frac{Z}{\frac{2\pi T_\perp}{m}\sqrt{\frac{2\pi T_\parallel}{m}}} \frac{2\pi B_b}{m} \int_{\boldsymbol{\nu}_i} \mathrm{d}\mu\, \mathrm{d}v_{\parallel b} \exp\left(-\frac{B_b \mu}{T_\perp}\right) \exp\left(-\frac{m v_{\parallel b}^2}{2T_\parallel}\right)$$

Static Vlasov Code

Time-independent distribution function [Chiu and Schulz, 1978]

→ $f(\boldsymbol{r}_b, \boldsymbol{v}_b) = f(\boldsymbol{r}_i, \boldsymbol{v}_i)$

$\boldsymbol{r}$: position vector

$\boldsymbol{\Omega}_i$: accessible velocity space @ point i

$\boldsymbol{\nu}_i$: accessible velocity space @ boundary

$$n_i = \int_{\boldsymbol{\Omega}_i} \mathrm{d}\boldsymbol{v}_i\, f(\boldsymbol{r}_i, \boldsymbol{v}_i) = \int_{\boldsymbol{\nu}_i} \mathrm{d}\boldsymbol{v}_b \left|\frac{\partial \boldsymbol{v}_i}{\partial \boldsymbol{v}_b}\right| f(\boldsymbol{r}_b, \boldsymbol{v}_b)$$

SVC integrate $f(\boldsymbol{r}_i, \boldsymbol{v}_i)$ over $\boldsymbol{\Omega}_i(\boldsymbol{v}_i)$ in velocity space at point i.

$$n_i = \frac{Z}{\frac{2\pi T_\perp}{m}\sqrt{\frac{2\pi T_\parallel}{m}}} \frac{2\pi B_i}{m} \int_{\boldsymbol{\Omega}_i} \mathrm{d}\mu\, \mathrm{d}v_{\parallel i} \exp\left(-\frac{B_b \mu}{T_\perp}\right) \exp\left(-\frac{m v_{\parallel b}^2}{2T_\parallel}\right)$$

3. Results

Initial condition

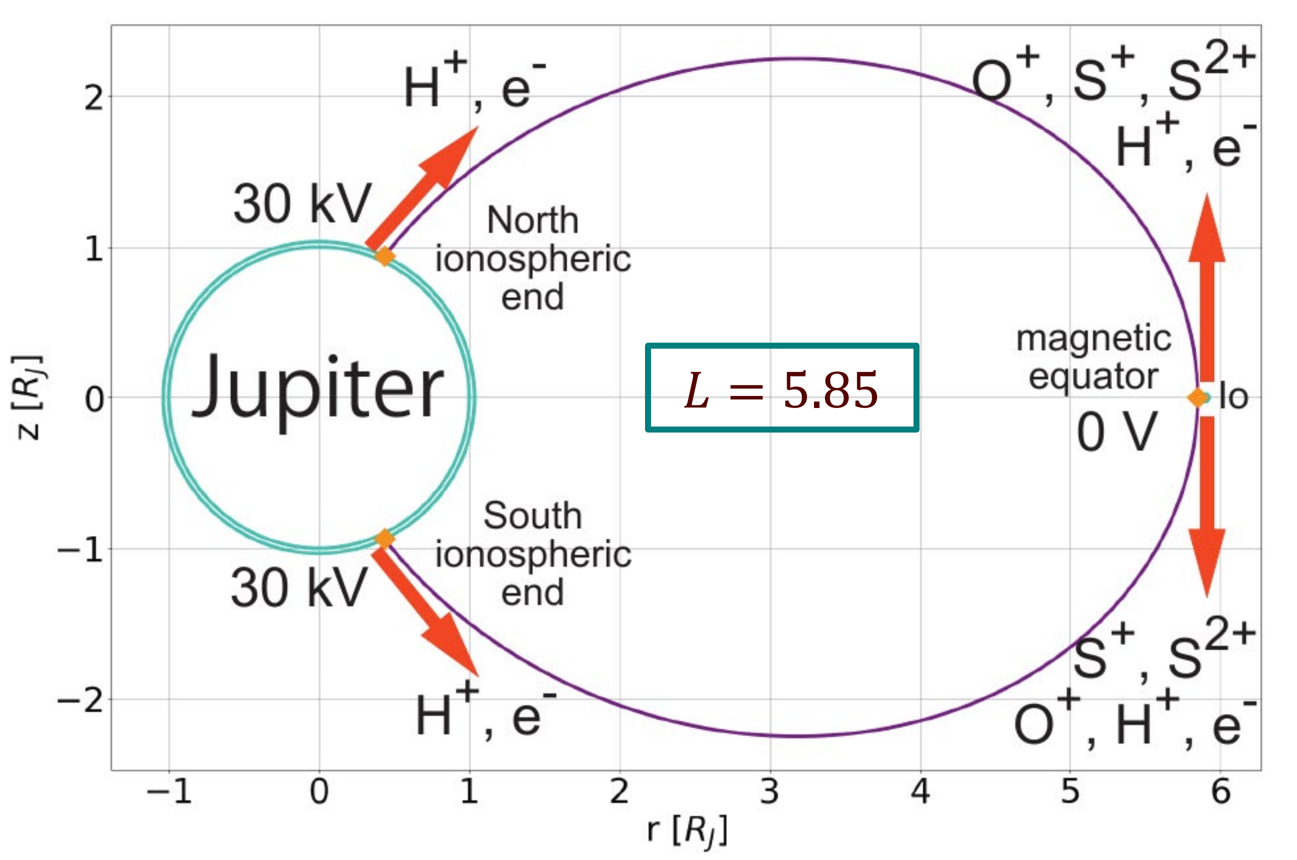

Initial electrostatic potential $\{\phi_i^0\}$ gap point

30 kV~26 kV: MLAT 64.63°~64.71°

26 kV~0 V: MLAT 54.54°~55.35°

boundary	s	Z_s [cm^{-3}]	$T_{\perp s} = T_{\parallel s}$ [eV]
Northern/ Southern ionospheric ends (Jupiter) Altitude: 2500 km	H^+	30000	0.1
	e^-		
Magnetic equator (Io)	O^+	1163	50
	S^+	291	
	S^{2+}	494	
	H^+	58	8.6
	cold e^-	2498	5
	hot e^-	2	200

Boundary condition is the same as Matsuda et al. (2010) SVC.

(MLAT: magnetic latitude)

number density n

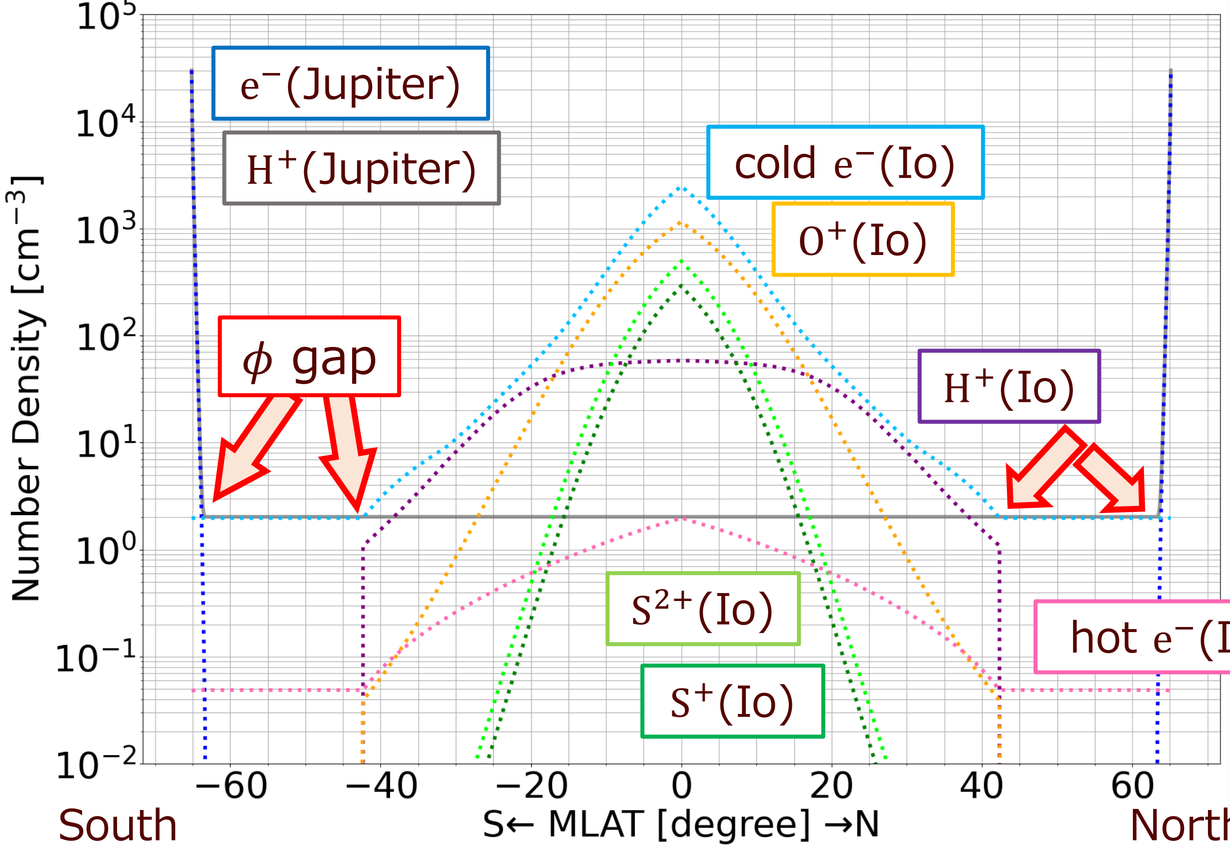

South ionospheric end

North ionospheric end

electrostatic potential ϕ

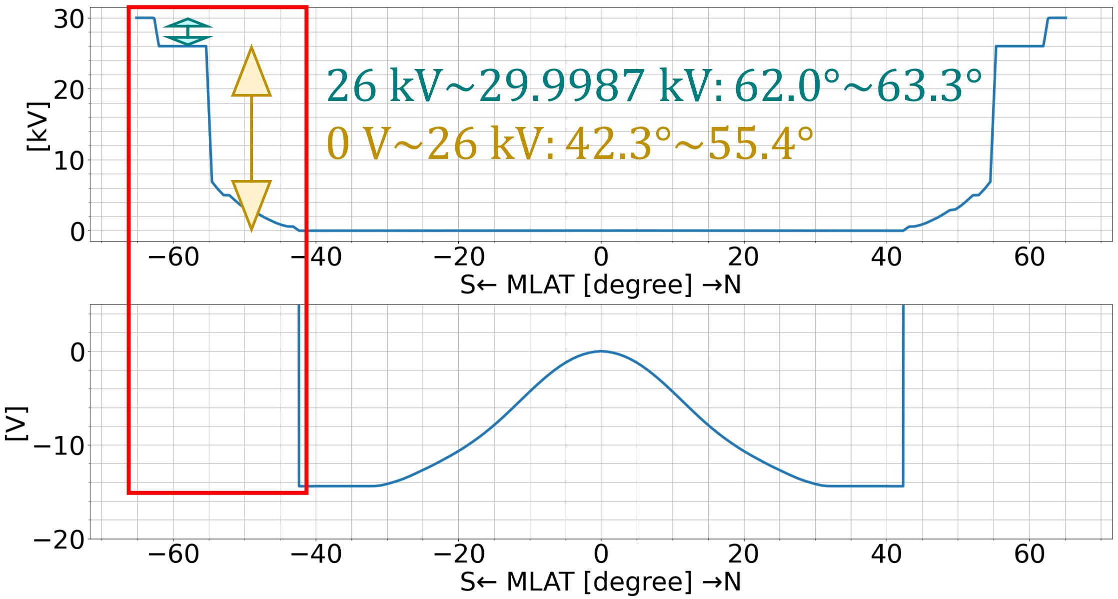

perpendicular pressure $P_\perp$

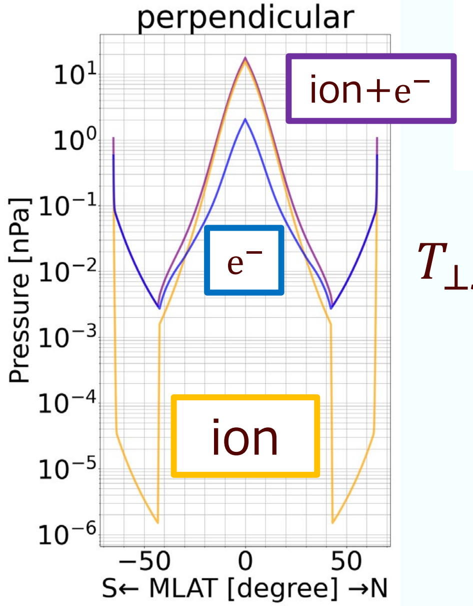

@ the potential gap
H^+(Jupiter) is accelerated
enough to reach the other boundary.

Between ϕ gaps, H^+ (Jupiter) & e^- (Io) only exist.

$T_{\perp s}$ (boundary)

H^+(Jupiter): 0.1 eV

e^- (Io): 5 eV & 200 eV

$\Rightarrow P_{\perp i} \ll P_{\perp e}$

4. Discussion

Comparison with Static Vlasov Code

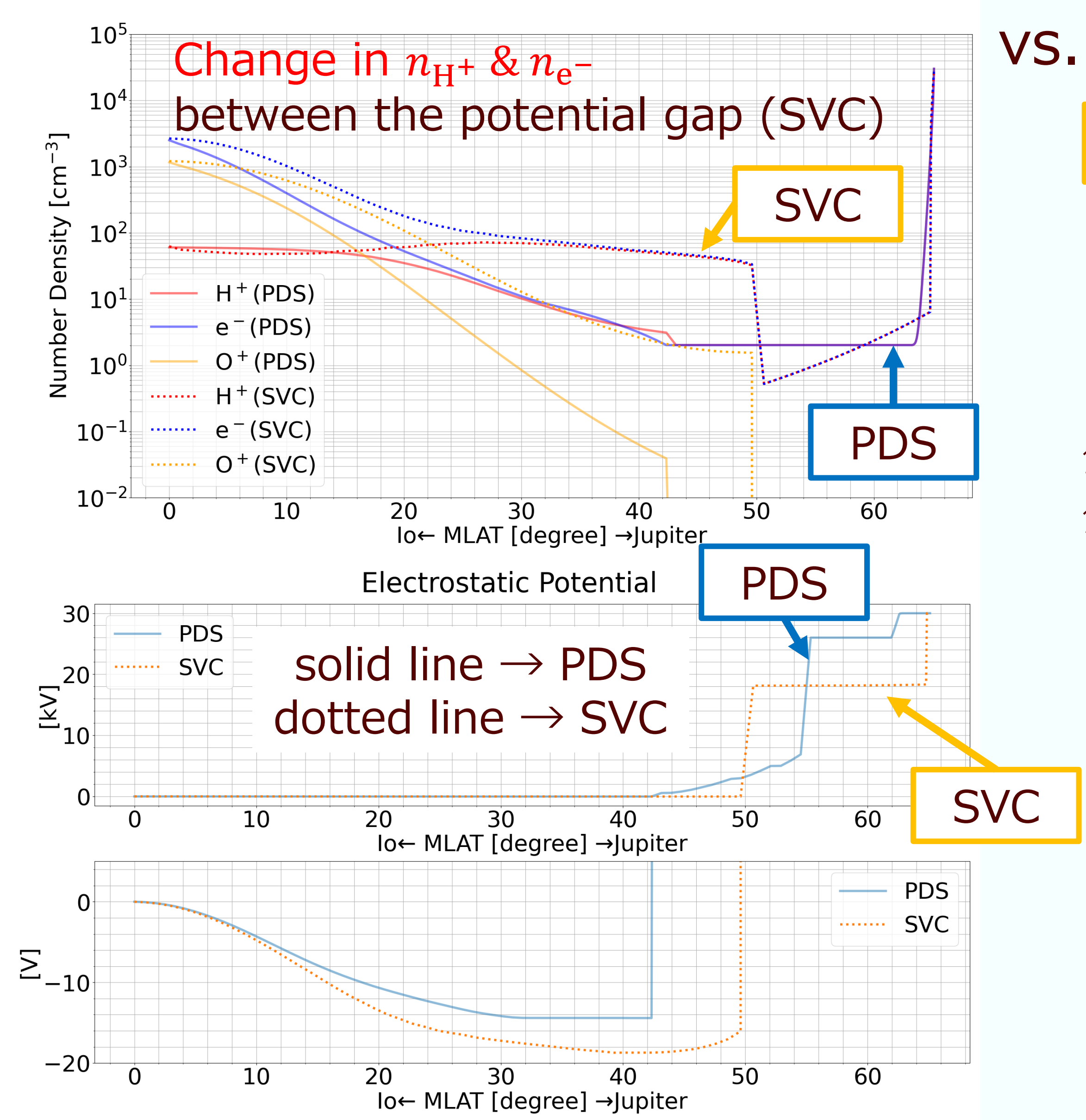

vs. Static Vlasov Code (SVC) [Matsuda et al. (2010)]

SVC

$$n_i = \frac{Z}{\frac{2\pi T_\perp}{m}\sqrt{\frac{2\pi T_\parallel}{m}}} \frac{2\pi B_i}{m} \int_{\Omega_i} \mathrm{d}\mu\, \mathrm{d}v_{\parallel i} \exp\left(-\frac{B_b \mu}{T_\perp}\right) \exp\left(-\frac{m v_{\parallel b}^2}{2T_\parallel}\right)$$

$\propto B_i$

n_i does not become small even at high latitudes.
n_i is variable between the potential gaps.

PDS

$$n_i = \frac{Z}{\frac{2\pi T_\perp}{m}\sqrt{\frac{2\pi T_\parallel}{m}}} \frac{2\pi B_b}{m} \int_{\nu_i} \mathrm{d}\mu\, \mathrm{d}v_{\parallel b} \exp\left(-\frac{B_b \mu}{T_\perp}\right) \exp\left(-\frac{m v_{\parallel b}^2}{2T_\parallel}\right)$$

Between 20° and 50°,
n_i of PDS is smaller than n_i of SVC.
n_i is constant between the potential gaps.

Applicable region and time scale

Applicable region

・collisionless ・stable

・homogeneously distribution across the magnetic field

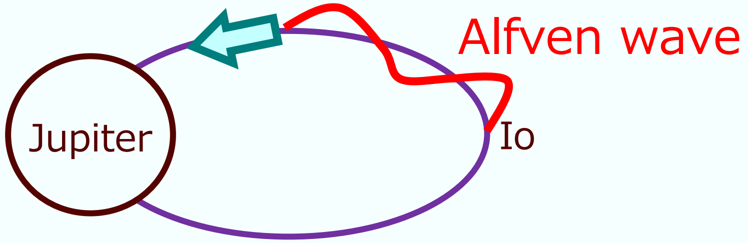

Applicable time scale

- must be smaller than the time scale on which the boundary conditions change

Jupiter rotates about 3.75° in the longitude direction during 370 sec. PDS

We need to assume that the conditions are stable.

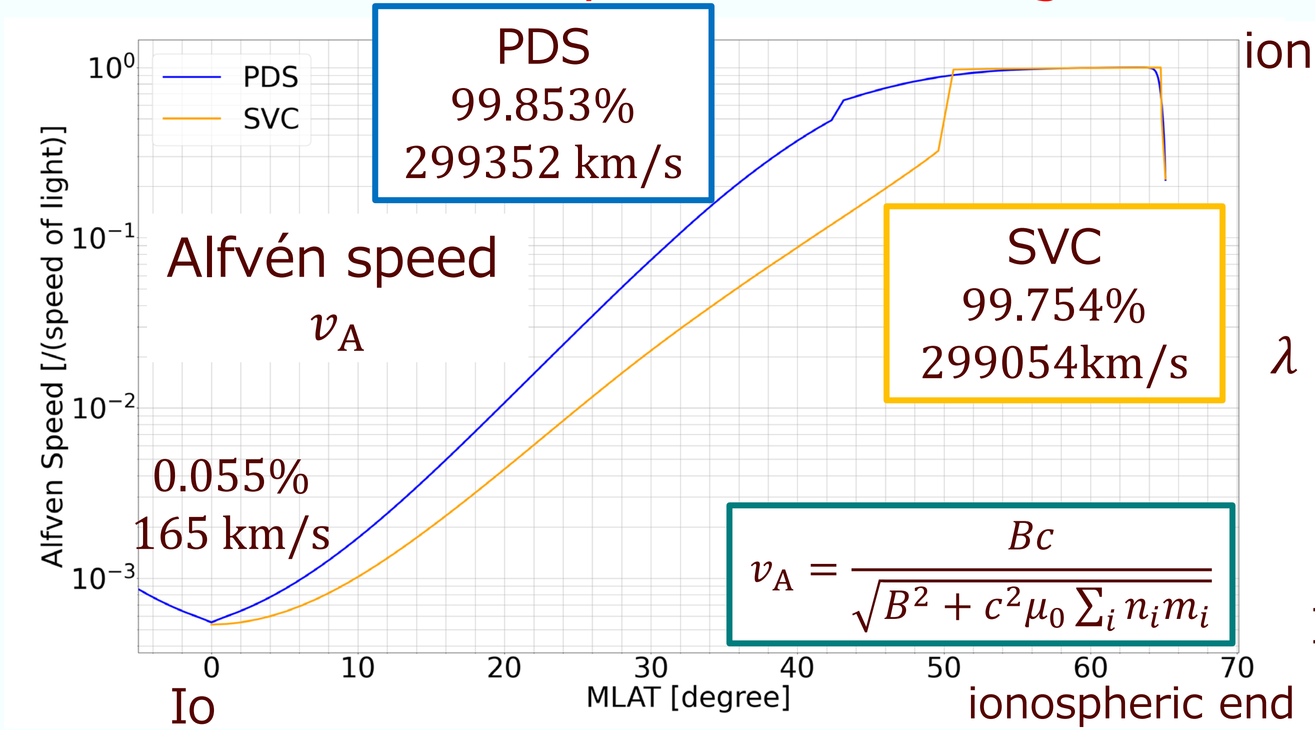

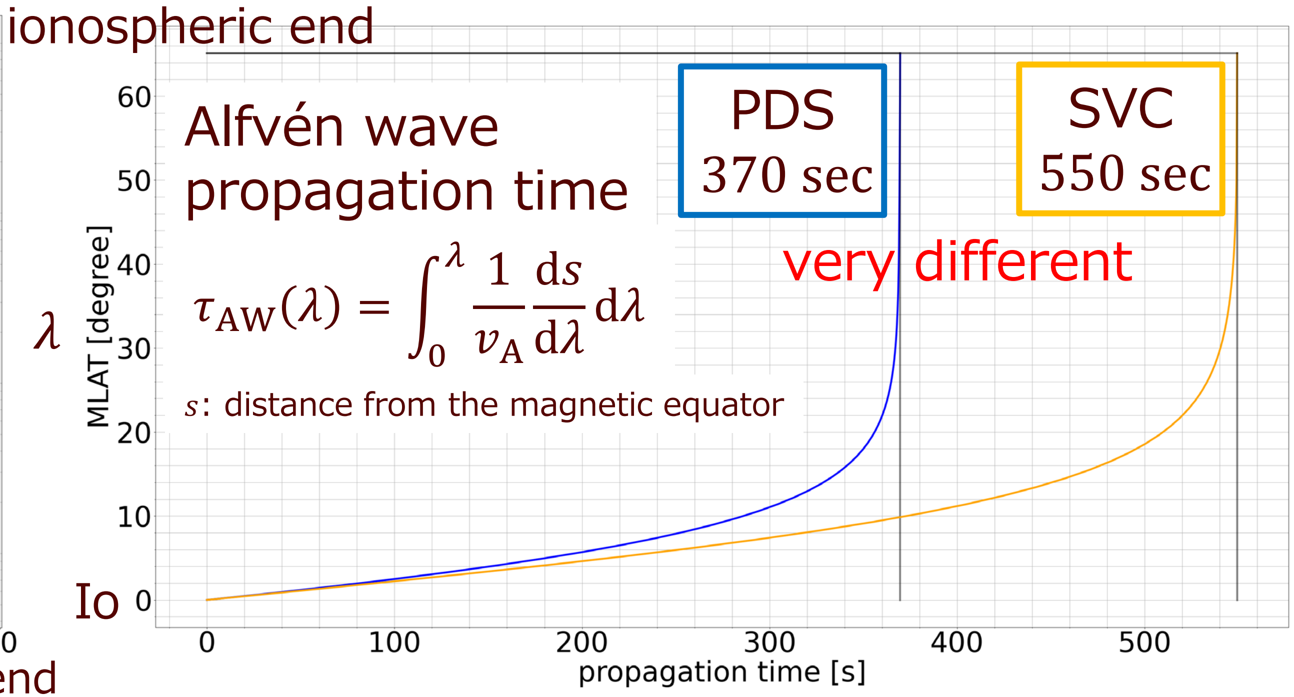

5. Summary

Summary

Developing a theoretical model to determine the mutually consistent number density and pressure spatial distributions. Purpose

- Developing the "Plasma Distribution Solver" (PDS) to calculate the field-aligned plasma profile by improving the Static Vlasov Code [e.g., Ergun et al., 2000] in handling the velocity distribution function.
- Applying PDS to the Jupiter-Io system (and terrestrial $L = 4$ magnetic field line in the thesis)
- Comparing with SVC: very different distribution results
- Evaluating applicable region and time scale
  - Time scale: We need to assume that the conditions are stable at least in the spatial extent corresponding to about $3.75°$ in the longitude direction during $370\,\mathrm{sec}$.

Ripple effect

Developing a theoretical model, "Plasma Distribution Solver (PDS)," to calculate the field-aligned plasma number density and pressure profiles.

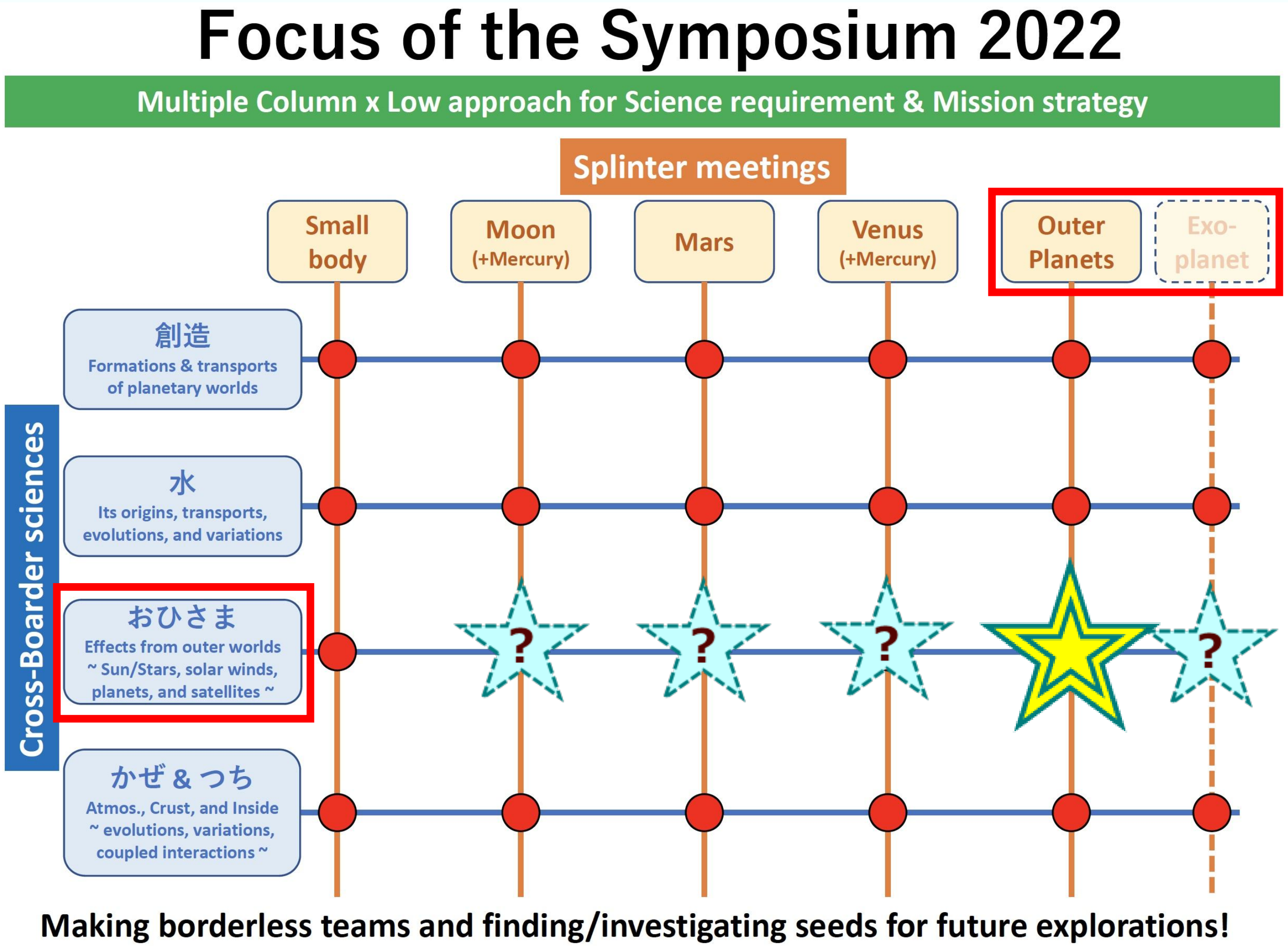

- velocity distribution function @ boundary
- initial electrostatic potential profile

↓

field-aligned profiles of

- number density n
- parallel mean flow velocity $V_{\parallel}$
- plasma pressure $P_{\perp}, P_{\parallel}, P$

↓

e.g.

- オーロラ電子加速過程の理解
  → 惑星大気の加熱
- 磁気圏-電離圏結合
  → 系外を含む惑星一般のプラズマ分布

Reference

- Chiu, Y. T., & Schulz, M. (1978). Self-consistent particle and parallel electrostatic field distributions in the magnetospheric-ionospheric auroral region. *Journal of Geophysical Research*, *83*(A2), 629–642. https://doi.org/10.1029/ja083ia02p00629
- Ergun, R. E., Carlson, C. W., McFadden, J. P., Mozer, F. S., & Strangeway, R. J. (2000). Parallel electric fields in discrete arcs. *Geophysical Research Letters*, *27*(24), 4053–4056. https://doi.org/10.1029/2000GL003819
- Matsuda, K., Misawa, H., Terada, N., & Katoh, Y. (2010). Asymmetrical features of frequency and intensity in the Io-related Jovian decametric radio sources: Modeling of the Io-Jupiter system. *Journal of Geophysical Research: Space Physics*, *115*(A12222). https://doi.org/10.1029/2010JA015844
- Mauk, B. H., Haggerty, D. K., Paranicas, C., Clark, G., Kollmann, P., Rymer, A. M., Bolton, S. J., Levin, S. M., Adriani, A., Allegrini, F., Bagenal, F., Bonfond, B., Connerney, J. E. P., Gladstone, G. R., Kurth, W. S., McComas, D. J., & Valek, P. (2017). Discrete and broadband electron acceleration in Jupiter's powerful aurora. *Nature*, *549*(7670), 66–69. https://doi.org/10.1038/nature23648
- Saur, J., Janser, S., Schreiner, A., Clark, G., Mauk, B. H., Kollmann, P., Ebert, R. W., Allegrini, F., Szalay, J. R., & Kotsiaros, S. (2018). Wave-Particle Interaction of Alfvén Waves in Jupiter's Magnetosphere: Auroral and Magnetospheric Particle Acceleration. *Journal of Geophysical Research: Space Physics*, *123*(11), 9560–9573. https://doi.org/10.1029/2018JA025948
- Streltsov, A., & Lotko, W. (1995). Dispersive field line resonances on auroral field lines. *Journal of Geophysical Research*, *100*(A10), 19457–19472. https://doi.org/10.1029/95JA01553
- Su, Y.-J., Ergun, R. E., Bagenal, F., & Delamere, P. A. (2003). Io-related Jovian auroral arcs: Modeling parallel electric fields. *Journal of Geophysical Research: Space Physics*, *108*(A2), 1094. https://doi.org/10.1029/2002JA009247
- Szalay, J. R., Bonfond, B., Allegrini, F., Bagenal, F., Bolton, S., Clark, G., Connerney, J. E. P., Ebert, R. W., Ergun, R. E., Gladstone, G. R., Grodent, D., Hospodarsky, G. B., Hue, V., Kurth, W. S., Kotsiaros, S., Levin, S. M., Louarn, P., Mauk, B., McComas, D. J., Saur, J., Valek, P. W., & Wilson, R. J. (2018). In Situ Observations Connected to the Io Footprint Tail Aurora. *Journal of Geophysical Research: Planets*, *123*(11), 3061–3077. https://doi.org/10.1029/2018JE005752

Appendix

Model and calculation method

Here, we check whether the charge density satisfies Poisson's equation.

$$\delta_i = \frac{(\rho_{\mathrm{d}\,i} - \rho_{\mathrm{P}\,i})^2}{|\rho_{\mathrm{d}-\,i}|\rho_{\mathrm{d}+\,i}}$$

$$\delta_{\mathrm{sum}} = \sqrt{\frac{1}{2N+1}\sum_{i=-N}^{N}\delta_i}$$

($\rho_{\mathrm{d}-}$, $\rho_{\mathrm{d}+}$: minus, plus charge density(ρ_{d}))

Iterate electrostatic potential $\{\phi_i\}$ using Newton method until δ_{sum} is sufficiently small.

$$\phi_i^{n+1} = \phi_i^n - \frac{\delta_i(\phi_i^n)}{\frac{\mathrm{d}}{\mathrm{d}\phi_i^n}\delta_i(\phi_i^n)}$$

(n: iteration number)

Initial electrostatic potential $\{\phi_i^0\}$

Potential energy U_{si}

$$\rho_{\mathrm{d}\,i} = \sum_s q_s \int\int_{\boldsymbol{v}_{si}} f_{sb}\, 2\pi v_{\perp b} \mathrm{d}v_{\parallel b} \mathrm{d}v_{\perp b}$$

$\rho_{\mathrm{P}\,i} = -\varepsilon_0 \Delta\phi_i$ (Poisson's eq.)

ε_0: electric constant

Is δ_{sum} sufficiently small?

NO

Iterating $\{\phi_i^n\}$ using Newton method

YES

$\{\phi_i\}$, $\{n_{si}\}$ are determined

Discussion: Centrifugal scale height model for the Io plasma torus

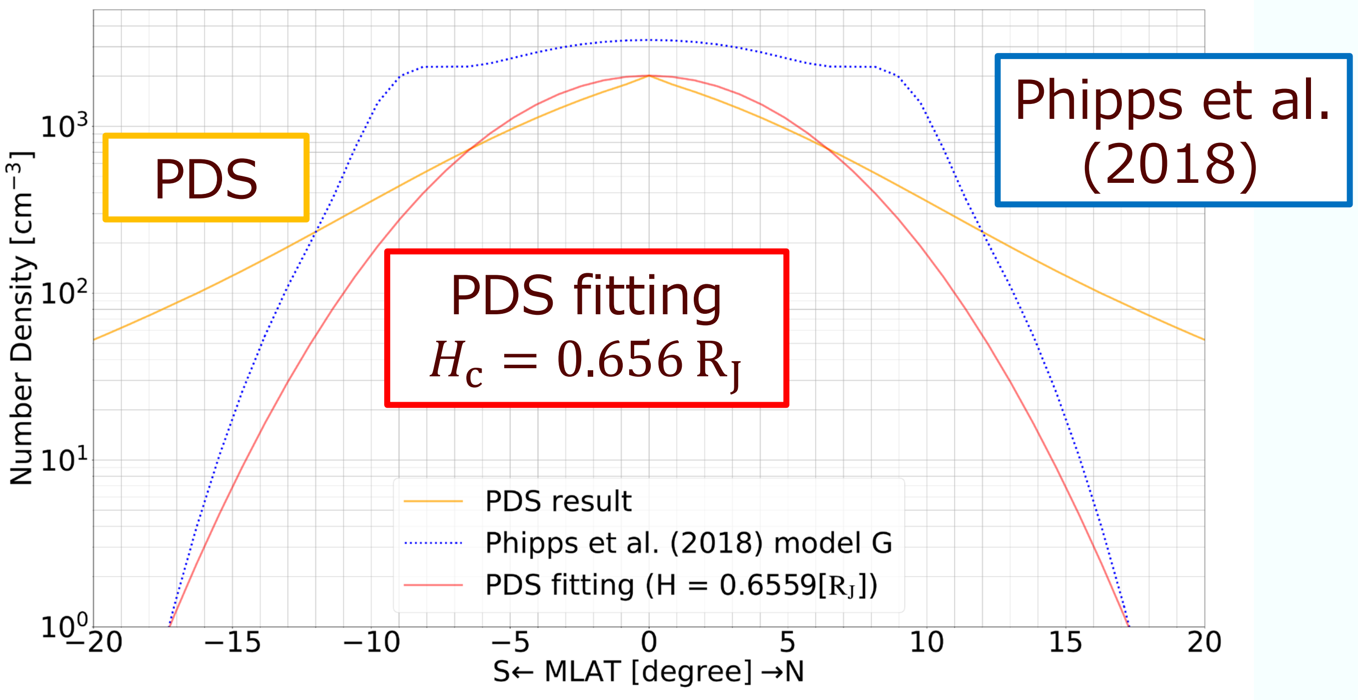

PDS: number density of Case J1

PDS fitting: fitting PDS within MLAT $\pm 20°$ with

$$n(z) = n_{eq} \exp\left(-\frac{z^2}{H_c^2}\right)$$

[e.g., Gledhill, 1967a,b]

by the least-squares method

coefficient of determination $= 0.917$

Phipps et al. (2018): empirical model by fitting the Juno's radio occultations results to the centrifugal scale height model

$H_c = 0.26\ R_J$ (Cold torus), $0.73\ R_J$ (Ribbon), $1.16\ R_J$ (Warm torus)

⇨ $H_c = 0.656\ R_J$ is close to $0.73\ R_J$ (Ribbon).

between MLAT $\pm 8°$: PDS close to PDS fitting and Phipps et al. (2018)

MLAT $> 10°$: difference becomes significant

(R_J: Jovian radius)

z: distance from the equatorial plane, H_c: centrifugal scale height, n_{eq}: number density at the equatorial plane

Results: plasma pressure

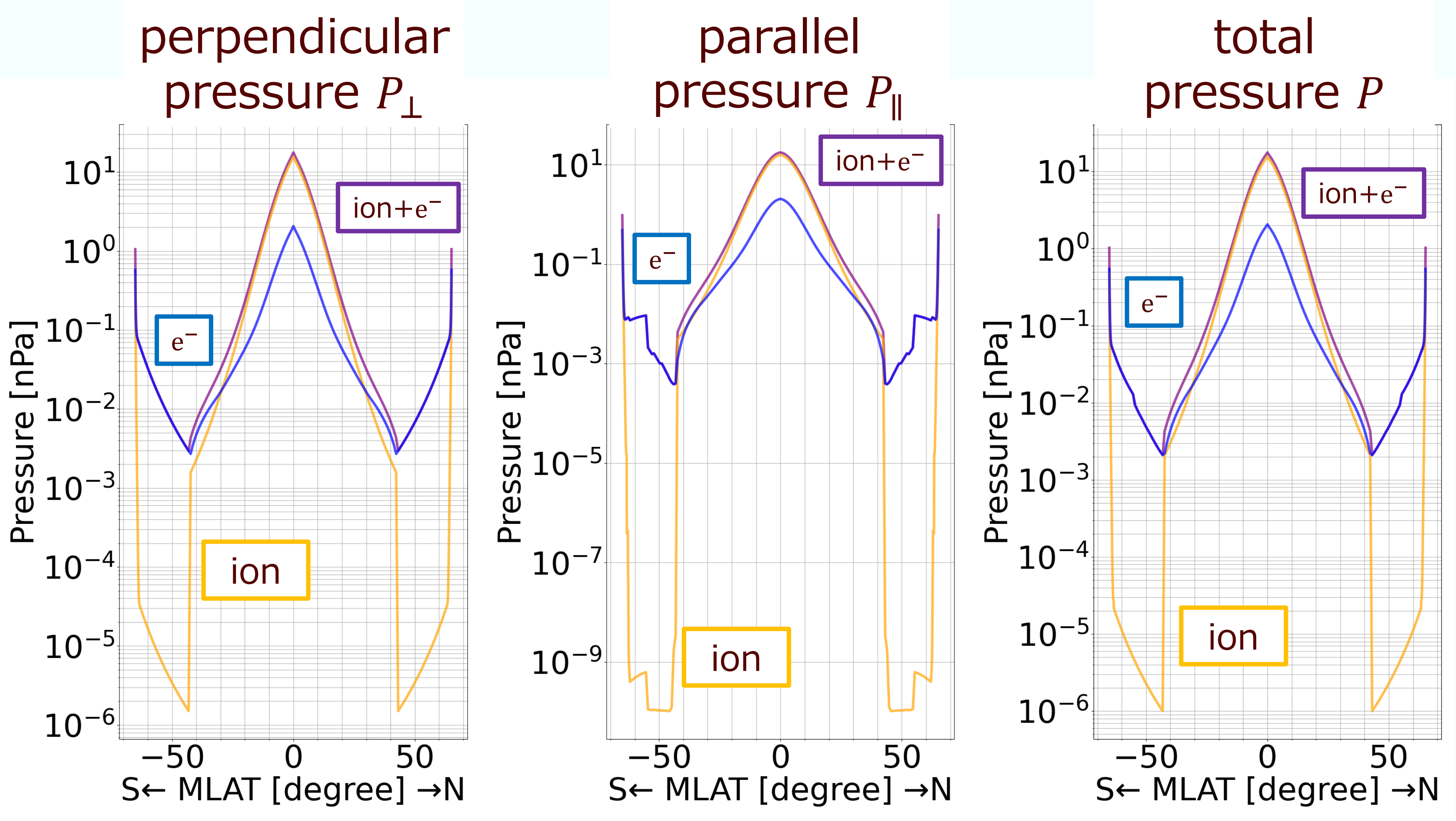

Results: current density

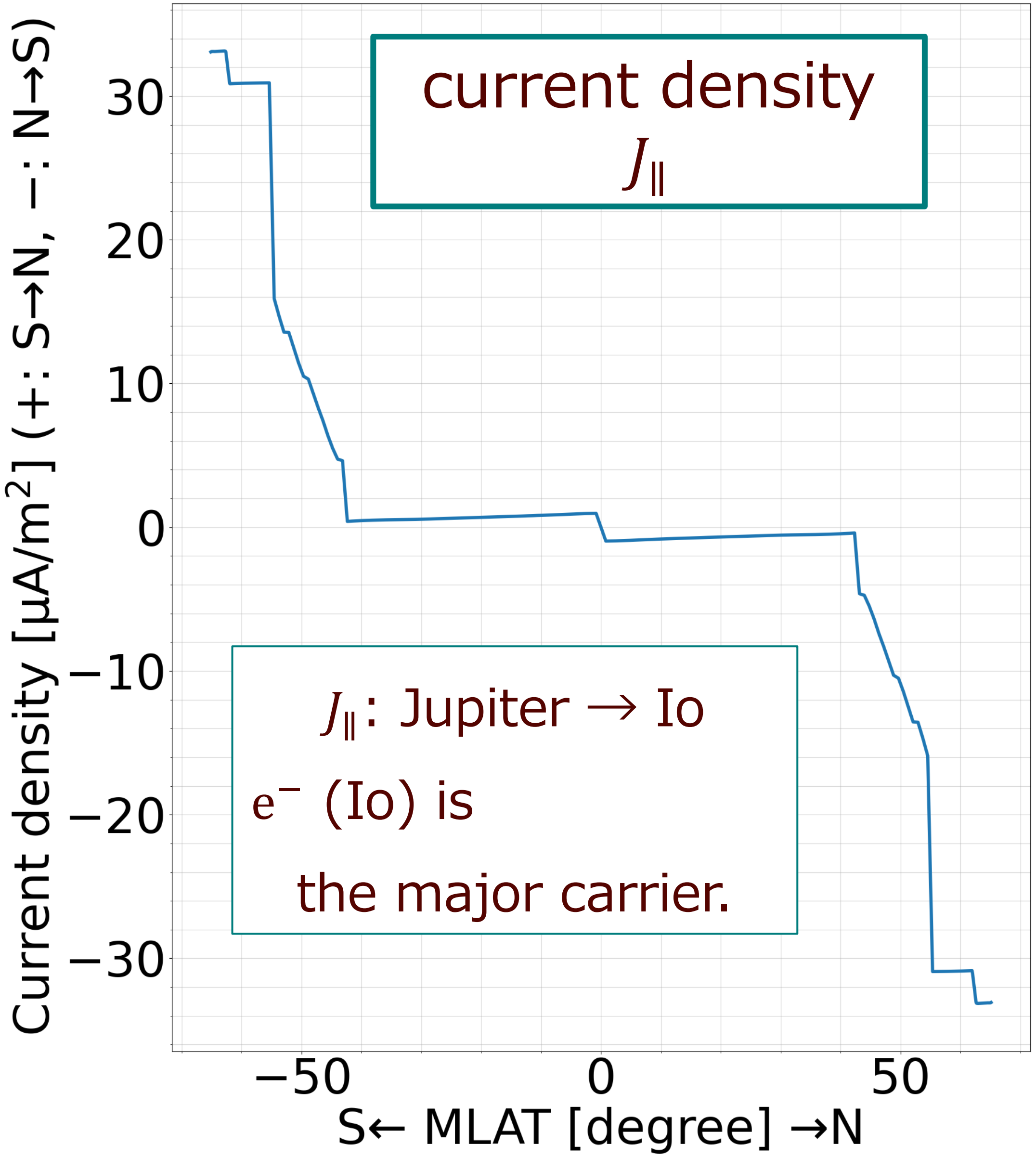

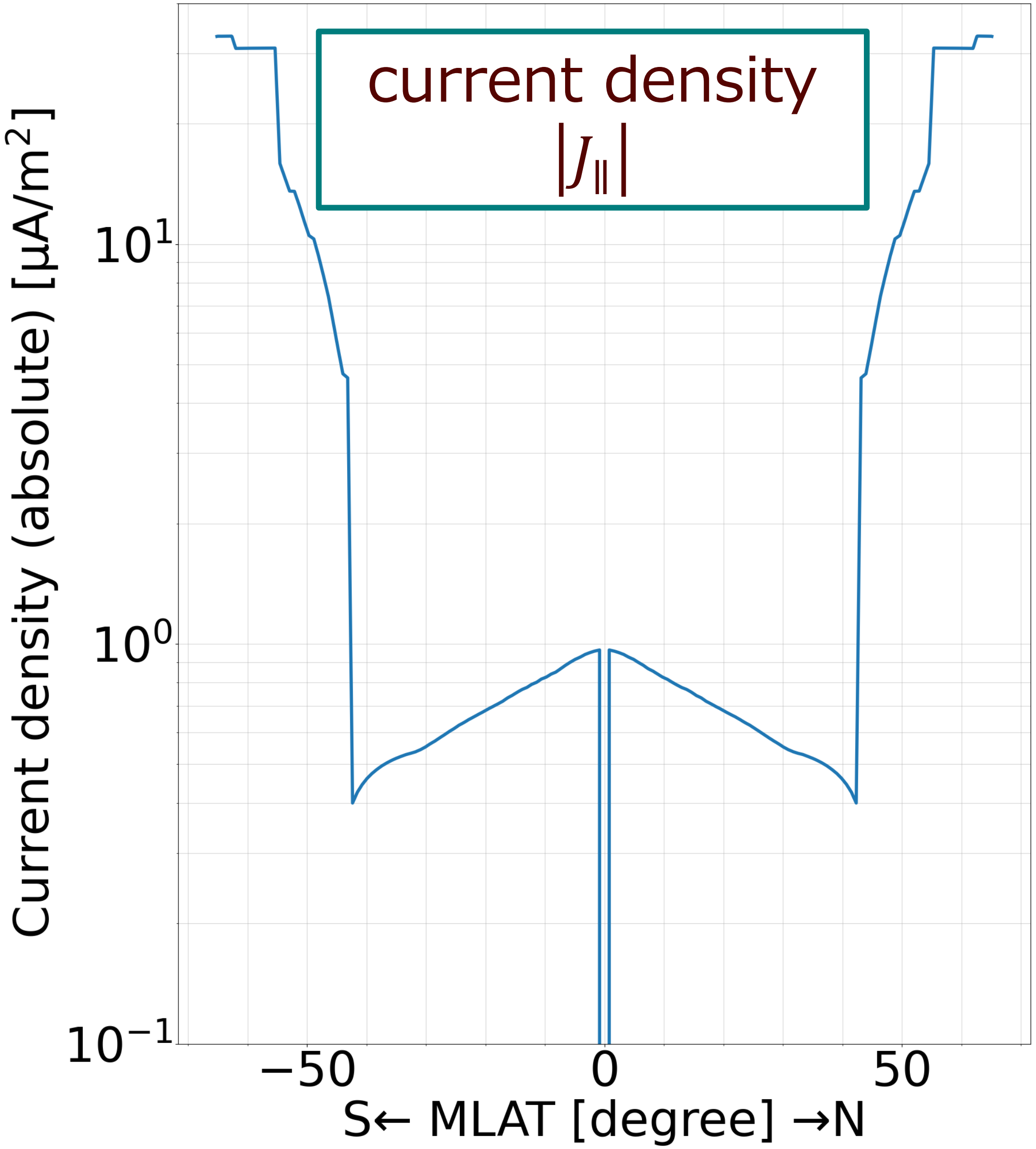

Characteristics of dispersive Alfvén waves

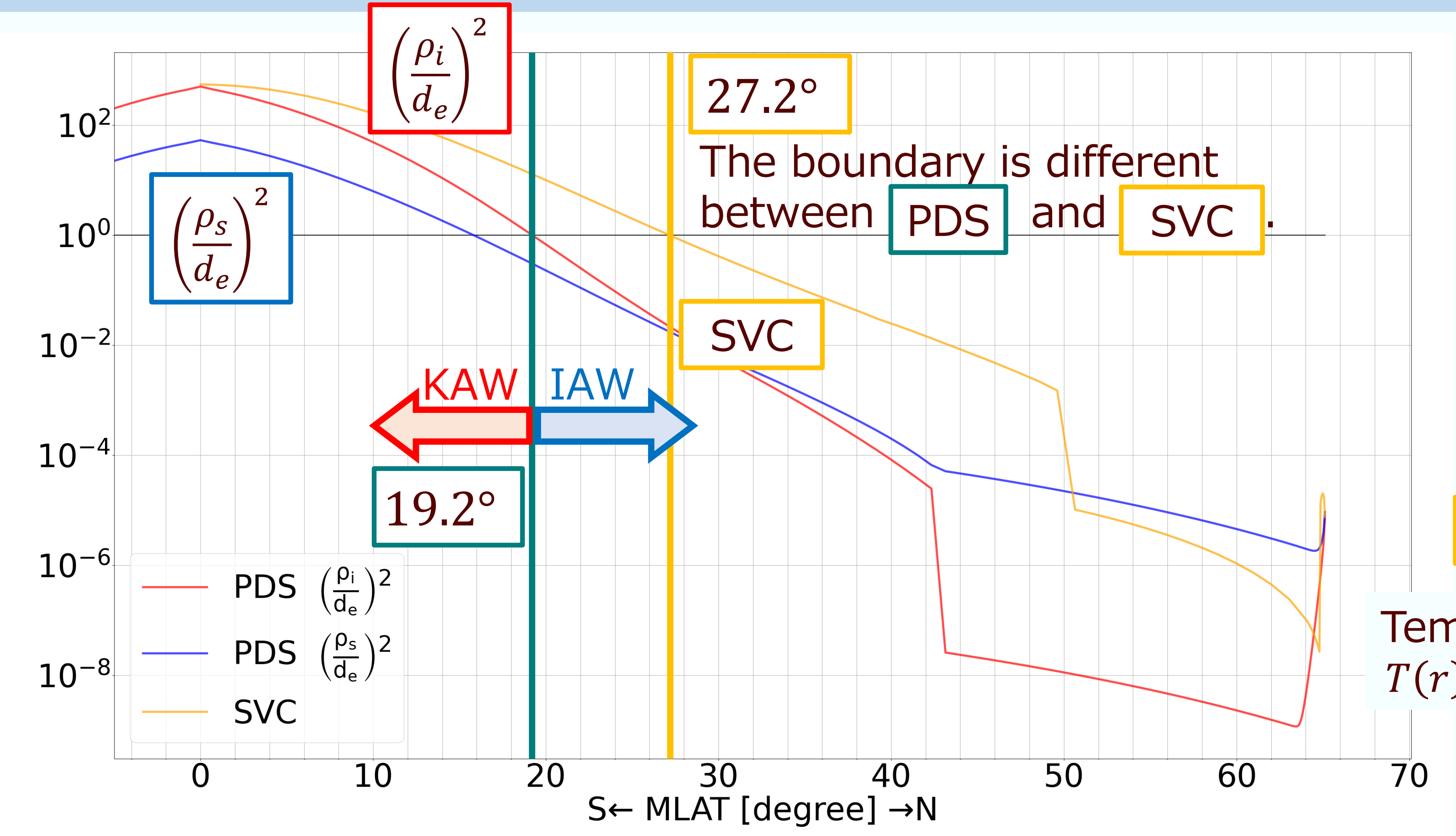

$$\left(\frac{\rho_i}{d_e}\right)^2 = \frac{1}{\zeta_i^2}\frac{N_e}{N_i}\frac{M_i}{m_e}\beta_{\perp i}$$

$$\left(\frac{\rho_s}{d_e}\right)^2 = \frac{1}{\zeta_i^2}\frac{M_i}{m_e}\beta_{\perp e}$$

either $\gg 1 \Rightarrow$ KAW
both $\ll 1 \Rightarrow$ IAW

SVC

Temperature function:
$T(r) = 0.1 + 49.9\tanh(r - r_{\mathrm{iono}})$

[Su et al., 2006]

ζ_i: average ion charge, $N_j = \sum_j n_j$: total number density, M_i: average ion mass, $\beta_{\perp j}$: perpendicular plasma beta,
$j = i$: for ion, $j = e$: for electron, $r\ [\mathrm{R_J}]$: distance along the field line from the Jovian center,
$r_{\mathrm{iono}}[\mathrm{R_J}]$: distance from the center to ionospheric end

Resonance velocity

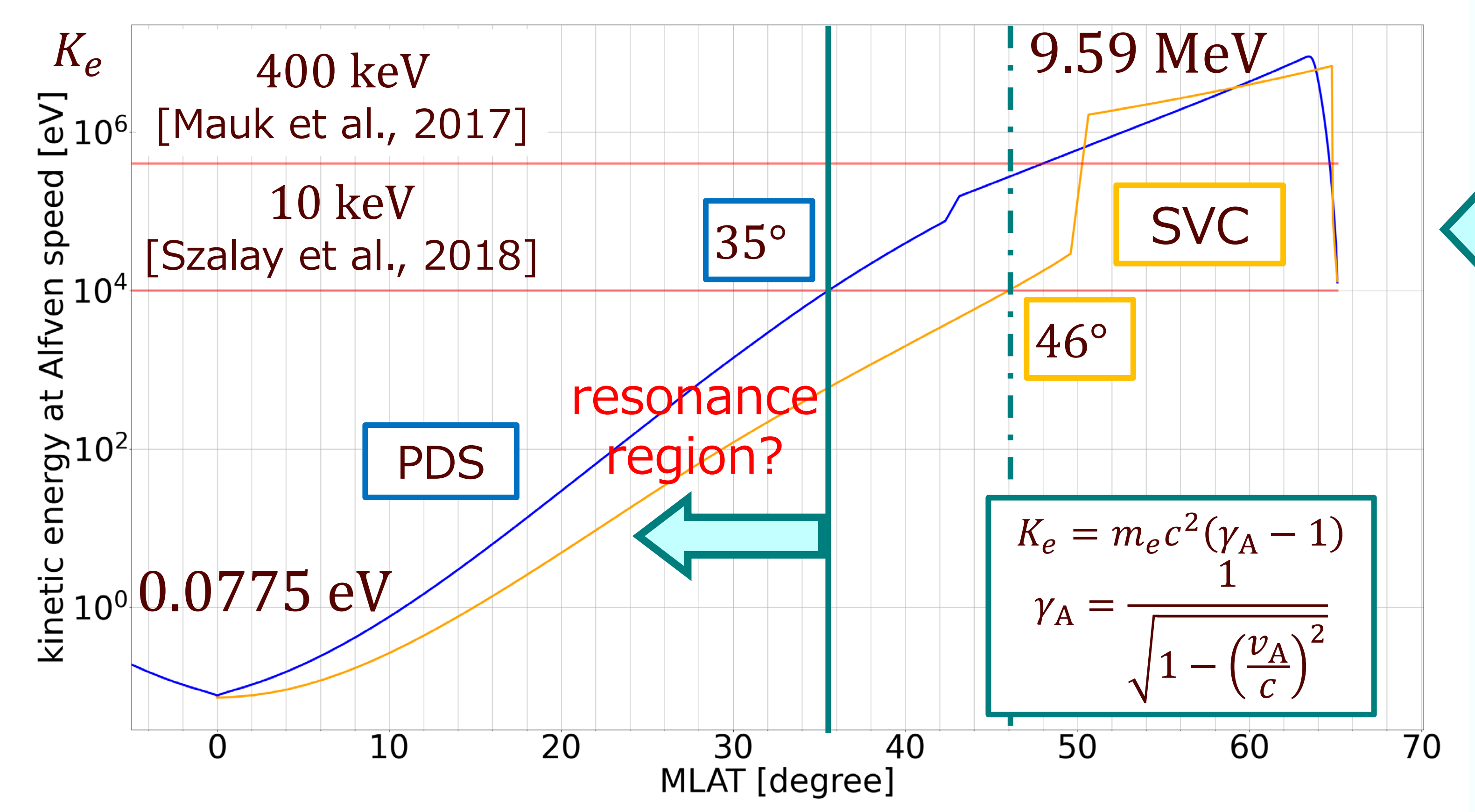

Dispersion relation: $\omega \sim k_\parallel v_A$

Landau damping: $\omega - k_\parallel v_\parallel = 0$

resonance velocity: $v_\parallel \sim v_A$

PDS

Electron acceleration by DAW may occur at MLAT $\lesssim 35°$?

SVC

Electron acceleration by DAW may occur at MLAT $\lesssim 46°$?